

Minimal-work protocols for inertial particles in non-harmonic traps

Julia Sanders,¹ Marco Baldovin,^{2,*} and Paolo Muratore-Ginanneschi¹

¹*Department of Mathematics and Statistics of the University of Helsinki, 00014 Helsinki, Finland*

²*Institute for Complex Systems, CNR, 00185, Rome, Italy*

(Dated: July 23, 2024)

The progress of miniaturized technology allows controlling physical systems at nanoscale with remarkable precision in regimes where thermal fluctuations are non-negligible. Experimental advancements have sparked interest in control problems in stochastic thermodynamics, typically concerning a time-dependent potential applied to a nanoparticle to reach a target stationary state in a given time with minimal energy cost. We study this problem for a particle subject to thermal fluctuations in a regime that takes into account the effects of inertia, and, building on the results of [1], provide a numerical method to find optimal controls even for non-Gaussian initial and final conditions corresponding to non-harmonic confinements. We show that the momentum mean tends to a constant value along the trajectory except at the boundary and the evolution of the variance is non-trivial. Our results also support that the lower bound on the optimal entropy production computed from the overdamped case is tight in the adiabatic limit.

Introduction — The past few years have seen growing interest in the experimental control of nanosystems [2–5]. Steering the state of a nanoscale device with high precision is intriguing for many reasons, in particular for information-technology applications [6–8]. For instance, a nanoparticle trapped in a bi-stable potential can model the minimal realization of an information bit: controlling nanoparticles in non-harmonic traps is therefore particularly interesting in the context of bit manipulation, specifically in the study of Landauer’s erasure problem [4, 9–13]. Considerable effort has been put into finding a theoretical solution to optimal control problems for physically relevant Markov models of the dynamics: overdamped [14–21], discrete configuration space jump [22–25], and underdamped [15, 26, 27] processes. In the underdamped case, however, besides harmonic confinements, a detailed quantitative understanding of optimality still poses an open question.

Motivated by the above, we search for protocols that steer a Brownian particle between two stationary end-states corresponding to different confining potentials while minimizing the average work. We consider the case of a particle subject to an underdamped dynamics characterized by small but non-negligible inertial effects. In Ref. [1], we map the problem into a system of two coupled partial differential equations, whose analytical solution is only available if the initial and final distributions of the stochastic particle are Gaussian (i.e., if the external potential fixing the boundary conditions is harmonic at the beginning and at the end of the protocol). Here, we discuss a numerical method for solving those equations for non-Gaussian boundary conditions. This gives an optimal solution to the problem for non-harmonic trapping potentials, including bi-stable potentials.

Optimization problem — Consider a classical particle of mass m , whose position and velocity along a given direction are denoted by q and p respectively. The particle

is subject to a frictional force $-p/\tau$ and thermal fluctuations at inverse temperature β . We also assume the presence of a time-dependent confining potential $U(q, t)$ that can be controlled externally. The dynamics read therefore

$$\dot{q} = \frac{p}{m} \quad (1a)$$

$$\dot{p} = -\frac{p}{\tau} - \partial_q U + \sqrt{\frac{2m}{\tau\beta}} \xi \quad (1b)$$

where $\xi(t)$ is a Gaussian white noise with zero mean and $\langle \xi(t)\xi(t') \rangle = \delta(t - t')$. At stationarity, the joint probability density function $f(q, p, t)$ of the particle’s position and momentum is

$$f_{eq}(q, p|U_{eq}) \propto \exp\left(-\beta\frac{p^2}{2m} - \beta U_{eq}(q)\right).$$

Controlling $U(q, t)$ allows us to modify the distribution of the system in time. We want to steer the state from an initial probability density function $f_{eq}(q, p|U_i)$ to a final one $f_{eq}(q, p|U_f)$ in a finite time t_f while minimizing the average external work done on the system

$$\langle W \rangle = \int_0^{t_f} dt \int dq dp \partial_t U(q, t) f(q, p, t). \quad (2)$$

Minimizing the average work between fixed states is equivalent to finding the protocol leading to the minimal average entropy production [17, 28]. The cost of the corresponding optimization problem is, however, non-convex in the control [15, 27]. Following the strategy of [27], it is therefore useful to consider a regularized version of the dynamics, characterized by the same stationary distribution:

$$\dot{q} = \frac{p}{m} - \frac{g\tau}{m} \partial_q U + \sqrt{\frac{2g\tau}{m\beta}} \eta \quad (3a)$$

$$\dot{p} = -\frac{p}{\tau} - \partial_q U + \sqrt{\frac{2m}{\tau\beta}} \xi \quad (3b)$$

* marco.baldovin@cnr.it

where $\eta(t)$ is a Gaussian white noise independent of $\xi(t)$, such that $\langle \eta(t)\eta(t') \rangle = \delta(t-t')$. The g is a regularizing constant. In the limit $g \rightarrow 0$, the dynamics (1) are recovered.

We address the problem within the mathematical framework of Pontryagin's theory [29, 30]. A perturbative solution can be found up to second order in powers of the dimensionless parameter

$$\varepsilon = \sqrt{\frac{\tau^2}{\beta \ell^2 m}}, \quad (4)$$

and a time horizon $t_f = O(\varepsilon^{-2})$. We assume ε to be much smaller than 1. Here, ℓ represents the characteristic length-scale of the model [31]. Finding the optimal control reduces to solving the ‘‘cell problem’’ in dimensionless variables

$$\partial_s \rho = \varepsilon^2 \partial_x \rho (\partial_x \sigma) \quad (5a)$$

$$\partial_s \sigma = \frac{\varepsilon^2}{2} (\partial_x \sigma)^2 \quad (5b)$$

for the (dimensionless) fields $\rho(x, s)$ and $\sigma(x, s)$, with boundary conditions given by

$$\rho(x, 0) = \frac{\exp(-\beta U_i(\ell x))}{\int_{\mathbb{R}} dy \exp(-\beta U_i(y))} \quad (6a)$$

$$\rho(x, t_f/\tau) = \frac{\exp(-\beta U_f(\ell x))}{\int_{\mathbb{R}} dy \exp(-\beta U_f(y))}. \quad (6b)$$

The field ρ is related to the solution of the optimal problem for an overdamped dynamics with the same boundary conditions [17]. For the precise relation with the quantities used in Ref. [1], see Appendix A. Once ρ and σ are found, the optimal control is computed as

$$U(q, t) \simeq -\frac{1}{\beta} \ln \rho(q/\ell, t/\tau) + c_1(t/\tau) \sigma(q/\ell, t/\tau) - c_2(t/\tau) q + O(\varepsilon) \quad (7)$$

and the marginal probability density function as

$$f(q, t) \simeq \frac{\rho(q/\ell, t/\tau)}{\ell} + \frac{\varepsilon^2}{\ell} f_2(q/\ell, t/\tau) + O(\varepsilon^3), \quad (8)$$

where the explicit forms of the functions c_1 , c_2 and f_2 are reported in Appendix B. The cost function, i.e. the average entropy production of the process, is given by

$$\mathcal{E} = \left\langle \ln \frac{f_{eq}(q, p|U_i)}{f_{eq}(q, p|U_f)} \right\rangle + \frac{1}{\tau} \int_0^{t_f} dt \left(\frac{\beta \langle p^2(t) \rangle}{m} - 1 \right) + \frac{g\tau}{m} \int_0^{t_f} dt \left\langle \beta (\partial_q U(t))^2 - \partial_q^2 U(t) \right\rangle. \quad (9)$$

The first term is the Gibbs-Shannon entropy variation between the end states, which is fixed by the boundary conditions. In the $g \ll 1$ limit the relevant part of

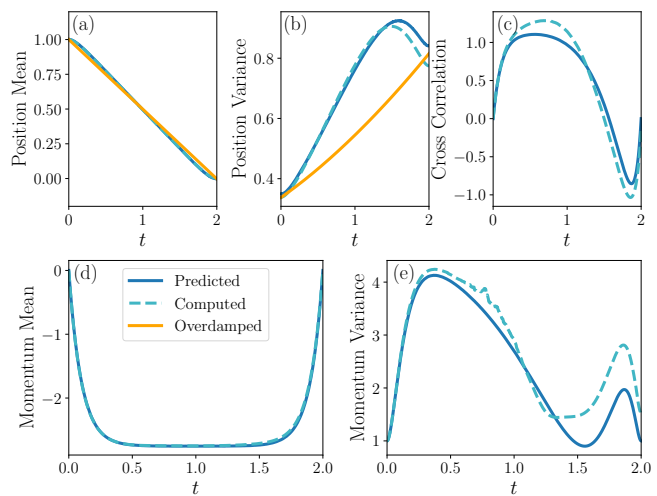


FIG. 1. Predictions for the first and second order cumulants of the position and variance processes in the underdamped dynamics, computed using expressions in Appendix B. The dashed line shows the cumulants computed along simulated trajectories of the dynamics (3) under the predicted optimal control protocol (7). We use the assigned initial distribution (6a) with $U_i(q) = (q-1)^4$ and assigned final distribution (6b) with $U_f(q) = (q^2-1)^2$. We use $t_f = 2$, $\varepsilon = 0.2$, $\tau = 1$, and $g = 0.01$. The cell problem (5) is solved numerically with $N = 25000$ independent sample positions in the interval $[-5, 5]$ from the initial and final distributions. The Burgers velocity σ is computed by (13) and intermediate densities ρ are estimated by kernel density estimation with an Epanechnikov kernel (12) and bandwidth $h = 0.15$. The time interval $[0, t_f]$ is discretized into increments of size 10^{-4} . The simulated trajectories of (3) use a total of 10^6 trajectories and the Euler-Maruyama scheme.

the cost comes from the second term, forcing the momentum variance to stay as close as possible to its equilibrium value. The average entropy production has its overdamped counterpart as a lower bound [1].

$$\mathcal{E} \geq \frac{\varepsilon^2}{1+g} \int_0^{t_f/\tau} ds \int_{\mathbb{R}} dx \rho(x, s) (\partial_x \sigma(x, s))^2 \quad (10)$$

Numerical method and results — Following Section V in [17], we know that the characteristics of the compressible Euler dynamics (5b) follow straight lines. Therefore, to find the solution numerically, N positions are sampled independently from the initial and final distributions, denoted $\{x_i^{(n)}\}_n$ and $\{x_f^{(n)}\}_n$ respectively, for $1 \leq n \leq N$. A matching is then found that minimizes the total squared distance between the two sets that preserves the ordering of points: if, for $n < m$, $x_i^{(n)} \leq x_i^{(m)}$ and $x_f^{(n)} \leq x_f^{(m)}$, then $x_i^{(n)}$ is matched with $x_f^{(n)}$. In the one dimensional case shown here, we use linear programming from the Python Optimal Transport library [32]. For higher dimensional problems it may be necessary to use computationally cheaper methods, such as the Sinkhorn algorithm (Chapter 4 of [33]), at the price of

an entropic regularization term. Matched end-points $x_i^{(n)}$ and $x_f^{(n)}$ are then used to obtain a discrete approximation of the Lagrangian map at any time t through a linear interpolation

$$x^{(n)}(t) = \frac{t_f - t}{t_f} x_i^{(n)} + \frac{t}{t_f} x_f^{(n)}. \quad (11)$$

The interpolation is performed for fixed times t in a discretization of $[0, t_f]$ and results in discretized sample trajectories of the position process. At each time, these are samples from the intermediate marginal density of the position and can be used to estimate the density ρ . We use kernel density estimation: a method of estimating distributions from an empirical set of samples and a smoothing parameter h (the bandwidth) [34]. An Epanechnikov kernel

$$K(x) = \begin{cases} \frac{3}{4}(1 - x^2) & \text{if } |x| \leq 1, \\ 0 & \text{otherwise} \end{cases} \quad (12)$$

is used [35]. The Burgers velocity is approximated by

$$-\partial\sigma(x^{(n)}(t), t/\tau) = \frac{\tau}{t_f} (x_f^{(n)} - x_i^{(n)}). \quad (13)$$

This is then interpolated into a function using a polynomial interpolation. The code implementing the procedure is available at [36].

The resulting fields ρ and σ are solutions of the cell problem (5). To find the corrections for the underdamped dynamics, we use the expressions detailed in Appendix B. In Fig. 1, we plot numerical predictions of the first and second order cumulants of the position and momentum in the underdamped dynamics (3). These are compared to simulated trajectories of the underdamped dynamics controlled by the predicted optimal control potential (7). The methods show good agreement and serve as a self-consistency check, with some deviation consistent with a perturbative regime. We also show, for comparison, the position mean and variance evolved by the overdamped dynamics. The position variance in the underdamped dynamics shows a distinct peak, a signature of inertial effects, which is not present in the overdamped dynamics.

Fig. 2 shows the predicted marginal densities of the position in the underdamped dynamics and the histogram of the evolved positions. Fig. 3 shows the total entropy production cost and the lower bound given by the overdamped dynamics at different values of final time t_f . This supports that the bound is tight in the adiabatic limit, as $t_f \rightarrow \infty$. To verify the consistency of the computations, we also plot the squared Wasserstein-2 distance between the assigned initial P_i and final P_f distributions (6)

$$\mathcal{W}_2^2(P_i, P_f) = \inf_{\pi} \int d\pi(x, y) (x - y)^2. \quad (14)$$

where π represents joint probability distributions whose marginal distribution of x is the assigned initial distribution and marginal distribution of y is the assigned final distribution [33]. This quantity is proportional to the

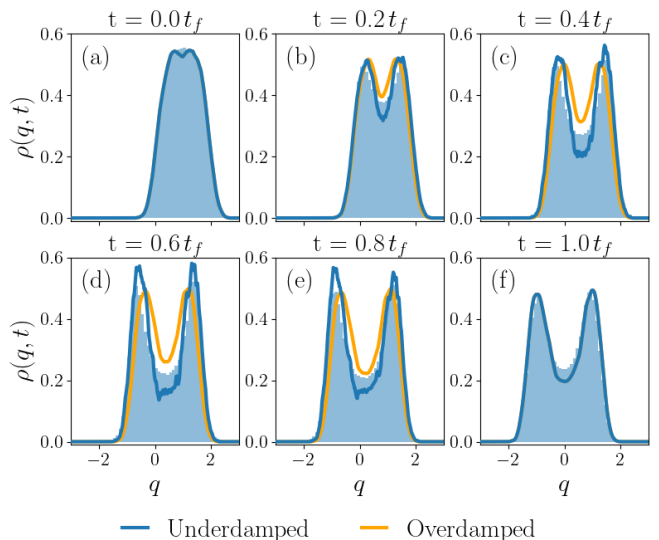


FIG. 2. Marginal density of the position in the underdamped (blue) and overdamped (orange) dynamics. Blue shaded regions in each panel show the histogram of points evolved by the underdamped dynamics (3) using the predicted optimal control protocol (7). We use $t_f = 2$, $\varepsilon = 0.2$, $\tau = 1$, and $g = 0.01$, and all other numerical parameters and assigned boundary conditions are used as in Fig. 1. Corrections to the density for the underdamped distribution are computed using Eq. (B11).

minimum entropy production in the overdamped dynamics by a factor depending on g and t_f , and has a finite limit as $g \rightarrow 0$ coinciding with that of (10) [1, 17].

Conclusions and outlook — In this letter, we apply the multiscale perturbation expansion around the overdamped limit developed in [1] to find minimal work protocols for inertial particles in non-harmonic traps. This approach allows us to make predictions for the optimal protocol and intermediate densities from its equivalent overdamped formulation, simplifying a complex numerical problem into the solution of the cell problem (5). This in turn can be solved using existing library implementations [32].

Our approach allows considering transitions between non-Gaussian boundary conditions in the underdamped dynamics. This is demonstrated numerically with boundary conditions modeling nucleation, where we can make predictions for the behavior of the first and second order cumulants of the momentum process, as well as the shape of the position marginal probability density function. Agreement between the theoretical expectations and numerical simulations obtained by applying the prescribed protocol confirms the reliability of our expansion. We use our method to compute the mean entropy production and verify the validity of the lower bounds provided in [1]. We also show that the inequality (10) is tight.

The effects of inertia and random noise cannot be ignored when designing electrical components at nanoscale. Understanding minimal work protocols for the erasure

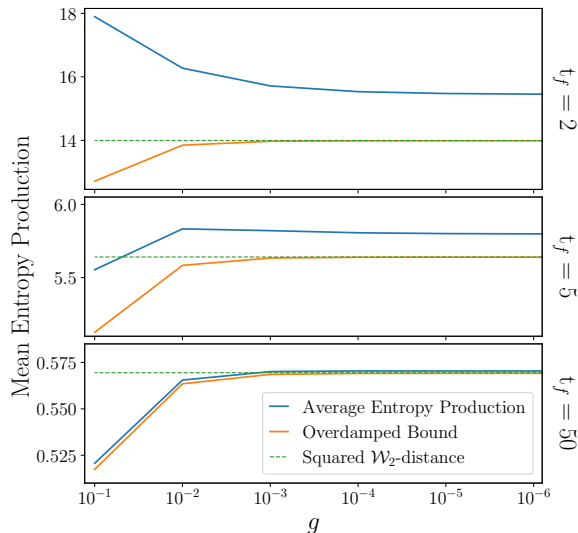


FIG. 3. Average entropy production (9) (blue) and the lower bound from the overdamped dynamics (10) (orange) computed at final times $t_f = 2$ (top), $t_f = 5$ (center) and $t_f = 50$ (bottom) for g decreasing along the horizontal axis. The squared \mathcal{W}_2 -distance (14) (green dashed) is a numerical estimate between the initial and final distributions computed using the Python Optimal Transport library [32]. The numerical parameters and boundary conditions are assigned as in Fig. 1. At $g = 10^{-6}$, the difference between the entropy production cost and the lower bound is approximately 1.5 for $t_f = 2$, approximately 0.16 for $t_f = 5$, and approximately $1.3 \cdot 10^{-3}$ for $t_f = 50$.

of one information bit in the underdamped dynamics is therefore important for improving the efficiency of computational devices, especially since these effects have been demonstrated to reduce the energy needed for bit operations [6, 7]. Control of underdamped processes may have applications even in other branches of science, for instance biological systems such as flocks of birds or self-propelled bacteria are subject to inertial effects [37, 38]. The application of control theory to such systems is a promising research line [39–41].

ACKNOWLEDGMENTS

MB was supported by ERC Advanced Grant RG.BIO (Contract No. 785932). JS was supported by a University of Helsinki funded doctoral researcher position, Doctoral Program in Mathematics and Statistics.

Appendix A: A note on notation

The notation of this letter differs slightly from that of [1], where the physical observables are expressed as functions of multiple time scales, as required by the

perturbative analysis. In this appendix, we provide a “Rosetta stone” to switch between the two notations. Quantities appearing in [1] are marked with tildes. The time scales transform as

$$\tilde{t}_0 = \frac{t}{\tau}, \quad \tilde{t}_2 = \varepsilon^2 \frac{t}{\tau}.$$

The fields solving the cell problem are related by

$$\tilde{\rho}_{\varepsilon^2 s}(x) = \rho(x, s), \quad \tilde{\sigma}_{\varepsilon^2 s}(x) = \sigma(x, s).$$

Averages $\langle \cdot \rangle$ in this paper are equivalent to $\tilde{\mathbb{E}}_{\mathcal{P}}(\cdot)$ there. For the position marginal distributions, one has

$$\tilde{f}_s(x) = \ell f(\ell x, \tau s), \quad \tilde{f}_{s, \varepsilon^2 s}^{(0:2)}(x) = f_2(x, s).$$

Appendix B: Analytic expressions

We provide here, for reference, explicit expressions for the coefficients c_1 and c_2 in Eq. (7), the first and second moments of the system’s distribution, and the leading correction to the position marginal probability density function. Explicit derivations can be found in [1].

We define two auxiliary functions

$$a(s) = 1 + \sinh(\omega s) \tanh \frac{\omega s_f}{2} - \cosh(\omega s) + b(s) \quad (\text{B1a})$$

$$b(s) = \frac{\omega e^{-s_f} (\cosh(\omega s) - e^{2s})}{\omega \cosh s_f - 2 \sinh s_f \coth \frac{\omega s_f}{2}} \quad (\text{B1b})$$

$$+ \frac{\omega e^{-s_f} (e^{2s_f} - \cosh(\omega s_f)) \sinh(\omega s)}{(\omega \cosh s_f - 2 \sinh s_f \coth \frac{\omega s_f}{2}) \sinh(\omega s_f)},$$

where $s_f = t_f/\tau$ and

$$\omega = \sqrt{\frac{1+g}{g}}.$$

Let us denote their integrals in $[0, s_f]$ as

$$A = \frac{1+g}{s_f} \int_0^{s_f} ds a(s) \quad (\text{B2a})$$

$$B = \frac{1+g}{s_f} \int_0^{s_f} ds b(s). \quad (\text{B2b})$$

It is also useful to introduce the mean and variance of the distribution ρ , namely

$$\mu(s) = \int_{\mathbb{R}} dx \rho(x, s) x \quad (\text{B3a})$$

$$v(s) = \int_{\mathbb{R}} dx \rho(x, s) x^2 - \mu(s)^2. \quad (\text{B3b})$$

It can be proven that

$$\mu'(s) = \frac{\tau}{t_f} \frac{\langle q \rangle_f - \langle q \rangle_\ell}{\ell},$$

where the averages $\langle \cdot \rangle_i$ and $\langle \cdot \rangle_f$ are computed over the initial and final state, respectively.

The two functions $c_1(t)$ and $c_2(t)$ appearing in Eq. (7) are given by

$$c_1 = \frac{1}{\beta} \frac{a' + a}{A} \quad (\text{B4a})$$

$$c_2 = \frac{m\ell}{\tau^2} \frac{B a' - A b' + B a - A b}{A(A - B)} \mu'(s), \quad (\text{B4b})$$

where the prime denotes a derivative with respect to the argument. Equipped with the above definitions, we can express the moments of the optimal process. When not specified, the functions a , b , μ , v and their derivatives are meant to depend on the rescaled time t/τ : we drop the explicit dependence to lighten the notation. The first moments are

$$\langle p(t) \rangle \simeq \frac{m\ell}{\tau} \frac{a - b}{A - B} \mu' + O(\varepsilon^2) \quad (\text{B5})$$

and

$$\begin{aligned} \langle q(t) \rangle &\simeq \ell \left(\mu - \frac{t}{\tau} \mu' \right) + \frac{g\tau}{m} \langle p(t) \rangle \\ &+ \frac{\ell(1+g)\mu'}{A-B} \int_0^{t/\tau} ds (a(s) - b(s)) + O(\varepsilon^3). \end{aligned} \quad (\text{B6})$$

The second moments read

$$\begin{aligned} \langle q(t)^2 \rangle - \langle q(t) \rangle^2 &\simeq \ell^2 v + \frac{g\ell^2}{A} a v' - \frac{t\ell^2}{\tau} v' \\ &+ \frac{1+g}{A} \ell^2 v' \int_0^{t/\tau} ds a(s) + O(\varepsilon^3), \end{aligned} \quad (\text{B7})$$

$$\begin{aligned} \langle p(t)^2 \rangle - \langle p(t) \rangle^2 &\simeq \frac{m}{\beta} - \frac{m^2 \ell^2 a^2 (\mu')^2}{\tau^2 A^2} \\ &+ \frac{a^2}{A^2} \frac{\tau^2}{\beta^2 \ell^2} \int_{\mathbb{R}} dx \rho(x, t/\tau) (\partial_x \sigma(x, t/\tau))^2 \\ &+ \frac{2}{A} \frac{\tau^2}{\beta^2 \ell^2} \int_0^{t/\tau} ds e^{-2(t/\tau-s)} a(s) \times \\ &\times \int_{\mathbb{R}} dx \rho(x, t/\tau) \partial_x^2 \sigma(x, t/\tau) + O(\varepsilon^3) \end{aligned} \quad (\text{B8})$$

and

$$\langle q(t)p(t) \rangle - \langle q(t) \rangle \langle p(t) \rangle \simeq \frac{\tau}{\beta} \frac{a}{2A} v' + O(\varepsilon^2). \quad (\text{B9})$$

By introducing the auxiliary field

$$\begin{aligned} f_1(x, s, s') &= -\frac{a(s)}{A} \rho(x, s') \partial_x \sigma(x, s') \\ &+ \frac{Ba(s) - Ab(s)}{\varepsilon^2 A(A - B)} \rho(x, s') \mu'(s'). \end{aligned} \quad (\text{B10})$$

we can finally express the leading correction to the marginal position probability density function as

$$\begin{aligned} f_2(x, t) &= -g \partial_x f_1(x, t/\tau, t/\tau) \\ &+ (1+g) \left(\frac{t}{t_f} \int_0^{t_f/\tau} ds - \int_0^{t/\tau} ds \right) \partial_x f_1(x, s, t/\tau). \end{aligned} \quad (\text{B11})$$

-
- [1] J. Sanders, M. Baldovin, and P. Muratore-Ginanneschi, Optimal control of underdamped systems: An analytic approach (2024), [arXiv:2403.00679 \[cond-mat.stat-mech\]](#).
- [2] I. A. Martínez, A. Petrosyan, D. Guéry-Odelin, E. Trizac, and S. Ciliberto, Engineered swift equilibration of a Brownian particle, *Nature Physics* **12**, 843–846 (2016).
- [3] C. Gonzalez-Ballester, M. Aspelmeyer, L. Novotny, R. Quidant, and O. Romero-Isart, Levitodynamics: Levitation and control of microscopic objects in vacuum, *Science* **374**, 10.1126/science.abg3027 (2021).
- [4] S. Dago and L. Bellon, Dynamics of information erasure and extension of Landauer’s bound to fast processes, *Phys. Rev. Lett.* **128**, 070604 (2022).
- [5] D. Raynal, T. de Guillebon, D. Guéry-Odelin, E. Trizac, J.-S. Lauret, and L. Rondin, Shortcuts to equilibrium with a levitated particle in the underdamped regime, *Physical Review Letters* **131**, 087101 (2023), 2303.09542.
- [6] M. López-Suárez, I. Neri, and L. Gammaioni, Sub-kb micro-electromechanical irreversible logic gate, *Nature communications* **7**, 12068 (2016).
- [7] A. Deshpande, M. Gopalkrishnan, T. E. Ouldrige, and N. S. Jones, Designing the optimal bit: balancing energetic cost, speed and reliability, *Proceedings of the Royal Society A: Mathematical, Physical and Engineering Sciences* **473**, 20170117 (2017).
- [8] M. A. Ciampini, T. Wenzl, M. Konopik, G. Thalhammer, M. Aspelmeyer, E. Lutz, and N. Kiesel, Experimental nonequilibrium memory erasure beyond Landauer’s bound (2021), [arXiv:2107.04429 \[cond-mat.stat-mech\]](#).
- [9] R. Landauer, Irreversibility and heat generation in the computing process, *IBM Journal of Research and Development* **5**, 183 (1961).
- [10] M. Esposito and C. V. den Broeck, Second law and Landauer principle far from equilibrium, *Europhysics Letters* **95**, 40004 (2011), 1104.5165.
- [11] A. Bérut, A. Arakelyan, A. Petrosyan, S. Ciliberto, R. Dillenschneider, and E. Lutz, Experimental verifica-

- tion of Landauer’s principle linking information and thermodynamics, *Nature* **483**, 187–189 (2012).
- [12] K. Proesmans, J. Ehrich, and J. Bechhoefer, Finite-Time Landauer Principle, *Physical Review Letters*, 100602 (2020).
- [13] S. Dago, J. Pereda, N. Barros, S. Ciliberto, and L. Bellon, Information and thermodynamics: fast and precise approach to Landauer’s bound in an underdamped micro-mechanical oscillator, *Physical Review Letters* **126**, 170601 (2021), arXiv:2102.09925 [cond-mat.stat-mech].
- [14] T. Schmiedl and U. Seifert, Optimal finite-time processes in stochastic thermodynamics, *Phys. Rev. Lett.* **98**, 108301 (2007).
- [15] A. Gomez-Marin, T. Schmiedl, and U. Seifert, Optimal protocols for minimal work processes in underdamped stochastic thermodynamics, *The Journal of Chemical Physics* **129**, 024114 (2008), arXiv:0803.0269 [cond-mat.stat-mech].
- [16] E. Aurell, C. Mejía-Monasterio, and P. Muratore-Ginanneschi, Optimal protocols and optimal transport in stochastic thermodynamics, *Physical Review Letters* **106**, 250601 (2011), arXiv:1012.2037 [cond-mat.stat-mech].
- [17] E. Aurell, K. Gawędzki, C. Mejía-Monasterio, R. Mohayae, and P. Muratore-Ginanneschi, Refined Second Law of Thermodynamics for fast random processes, *Journal of Statistical Physics* **147**, 487 (2012), arXiv:1201.3207 [cond-mat.stat-mech].
- [18] M. Baldovin, D. Guéry-Odelin, and E. Trizac, Shortcuts to adiabaticity for Lévy processes in harmonic traps, *Physical Review E* **106**, 054122 (2022).
- [19] D. Guéry-Odelin, C. Jarzynski, C. A. Plata, A. Prados, and E. Trizac, Driving rapidly while remaining in control: classical shortcuts from Hamiltonian to stochastic dynamics, *Reports on Progress in Physics* **86**, 035902 (2023).
- [20] S. Chennakesavalu and G. M. Rotskoff, Unified, Geometric Framework for Nonequilibrium Protocol Optimization, *Physical Review Letters* **130**, 10.1103/physrevlett.130.107101 (2023).
- [21] S. A. Loos, S. Monter, F. Ginot, and C. Bechinger, Universal symmetry of optimal control at the microscale, *Physical Review X* **14**, 021032 (2024).
- [22] M. Esposito, R. Kawai, K. Lindenberg, and C. Van den Broeck, Finite-time thermodynamics for a single-level quantum dot, *EPL (Europhysics Letters)* **89**, 20003 (2010), 0909.3618.
- [23] P. Muratore-Ginanneschi, C. Mejía-Monasterio, and L. Peliti, Heat release by controlled continuous-time Markov jump processes, *Journal of Statistical Physics* **150**, 181 (2013), arXiv:1203.4062 [cond-mat.stat-mech].
- [24] B. Remlein and U. Seifert, Optimality of nonconservative driving for finite-time processes with discrete states, *Physical Review E* **103**, 10.1103/physreve.103.1050105 (2021), 2103.08376.
- [25] A. Dechant, Minimum entropy production, detailed balance and Wasserstein distance for continuous-time Markov processes, *Journal of Physics A: Mathematical and Theoretical* **55**, 094001 (2022), 2110.01141.
- [26] P. Muratore-Ginanneschi, On extremals of the entropy production by “Langevin–Kramers” dynamics, *Journal of Statistical Mechanics: Theory and Experiment* **2014**, P05013 (2014), arXiv:1401.3394 [cond-mat.stat-mech].
- [27] P. Muratore-Ginanneschi and K. Schwieger, How nanomechanical systems can minimize dissipation, *Physical Review E* **90**, 060102(R) (2014), arXiv:1408.5298 [cond-mat.stat-mech].
- [28] L. Peliti and S. Pigolotti, *Stochastic Thermodynamics* (Princeton University Press, 2020).
- [29] D. E. Kirk, *Optimal control theory: an introduction* (Courier Corporation, 2004).
- [30] J. Bechhoefer, *Control Theory for Physicists* (Cambridge University Press, 2021).
- [31] E.g., $\ell = \sqrt{\langle q^2 \rangle_t - \langle q \rangle_t^2}$, where the averages are computed with respect to the initial state.
- [32] R. Flamary, N. Courty, A. Gramfort, M. Z. Alaya, A. Boisbunon, S. Chambon, L. Chapel, A. Corenflos, K. Fatras, N. Fournier, L. Gautheron, N. T. Gayraud, H. Janati, A. Rakotomamonjy, I. Redko, A. Rolet, A. Schutz, V. Seguy, D. J. Sutherland, R. Tavenard, A. Tong, and T. Vayer, Pot: Python optimal transport, *Journal of Machine Learning Research* **22**, 1 (2021).
- [33] G. Peyré, M. Cuturi, *et al.*, Computational optimal transport: With applications to data science, *Foundations and Trends® in Machine Learning* **11**, 355 (2019).
- [34] T. Hastie, R. Tibshirani, and J. Friedman, *The Elements of Statistical Learning: Data Mining, Inference, and Prediction* (Springer-Verlag, 2017).
- [35] F. Pedregosa, G. Varoquaux, A. Gramfort, V. Michel, B. Thirion, O. Grisel, M. Blondel, P. Prettenhofer, R. Weiss, V. Dubourg, J. Vanderplas, A. Passos, D. Cournapeau, M. Brucher, M. Perrot, and E. Duchesnay, Scikit-learn: Machine learning in Python, *Journal of Machine Learning Research* **12**, 2825 (2011).
- [36] <https://github.com/julia-sand/entropyproduction>.
- [37] A. Attanasi, A. Cavagna, L. Del Castello, I. Giardina, T. S. Grigera, A. Jelić, S. Melillo, L. Parisi, O. Pohl, E. Shen, and M. Viale, Information transfer and behavioural inertia in starling flocks, *Nature Physics* **10**, 691–696 (2014).
- [38] C. Scholz, S. Jahanshahi, A. Ldov, and H. Löwen, Inertial delay of self-propelled particles, *Nature Communications* **9**, 10.1038/s41467-018-07596-x (2018).
- [39] S. Shankar, V. Raju, and L. Mahadevan, Optimal transport and control of active drops, *Proceedings of the National Academy of Sciences* **119**, 10.1073/pnas.2121985119 (2022).
- [40] M. Baldovin, D. Guéry-Odelin, and E. Trizac, Control of active brownian particles: An exact solution, *Phys. Rev. Lett.* **131**, 118302 (2023).
- [41] L. K. Davis, K. Proesmans, and E. Fodor, Active matter under control: Insights from response theory, *Phys. Rev. X* **14**, 011012 (2024).